Journal of Applied Electrochemistry (2006) 36:1027–1034
DOI 10.1007/s10800-006-9153-8

Mechanistic study of the electropolymeric synthesis of a conducting polyacetylene chloride polymer

AI-LIN SHEN and TSE-CHUAN CHOU*
Department of Chemical Engineering, National Cheng Kung University, No. 1, Ta-Hsueh Road, Tainan, 701, Taiwan, ROC
*(*author for correspondence, tel.: +886-6-2757575-62639, fax: +886-6-2366836, e-mail: tcchou@mail.ncku.edu.tw)*

Received 12 September 2005; accepted in revised form 2 May 2006

Key words: conducting polymer, electropolymerization, mechanism, polyacetylene chloride, synthesis

Abstract

A conducting polyacetylene chloride polymer was synthesized by the electropolymerization of trichloroethylene, using the monomer in a concentration range from 0.0025 to 0.04 M, with 1.8 to 2.1 V vs. Ag/Ag^+ applied potential, and tetrabutylammonium perchlorate (0.1 M) and the organic electrolyte tetrabutylammonium tetrafluoroborate (0.01 M) in acetonitrile (50 ml), with mild agitation at room temperature. The electropolymerization was found to have several reaction steps in a paired electrolysis system. A reaction mechanism is proposed and a descriptive mathematical function was developed into a theoretical analysis, which correlates well with the experimental results. The rate determining step was found to be the separation of the Cl^- ion. The paired electrolysis current of trichloroethylene (TCE) can be expressed by the following function:

$$\frac{1}{i} = 0.0497\frac{1}{[\mathrm{TCE}]} + 66.92\frac{1}{X}.$$

where X is $\exp(-\beta_2 F\eta_2/RT)$ and β_2 and η_2 represent a transfer constant and the overpotential.

Nomenclature

A	variable defined by Equation (52)
C_t	the total active sites on the cathodic surface
C_v	unoccupied active site of the cathodic surface which is not covered by any adsorbing species.
F	Faraday constant, 96487 C mol^{-1}
i	total current density of the cell, A cm^{-2}
i_2, i_3, and i_i	the current of reaction step (2), (3), and chain initiation
$i_{2,0}$, $i_{3,0}$, and $i_{i,0}$	the exchange current of reaction step (2), (3), and chain initiation
k_1, k_2 etc.	ratio constant of reaction step (1), (2) etc.
k_{-1}, k_{-2} etc.	the backward ratio constant of reaction step (1), (2) etc.
M	acetylene chloride
$N^{\cdot}$	radical form defined by Equation (25)
$NM^{\cdot}_n$	radical form defined by Equation (28)
$NM_{n+m}N$	polymer defined by Equation (29)
NN	acetylene dichloride
$\overline{N^{\cdot}}$	dimensionless variable defined by Equation (37)
P	variable defined by Equation (37)
R	gas law constant, 8.314 J mol^{-1} K^{-1}
R_1	molecule form of trichloroethylene
R_{1s}	molecule form of trichloroethylene which was adsorbed on the surface of cathode
R_{2s}	ion form of trichloroethylene which was adsorbed an electron on the surface of cathode
R_{3s}	ion form of dichloroethylene which was adsorbed on the surface of cathode
R_4	ion form of acetylene chloride which was lost a hydrogen ion
$\overline{R_{1s}}$	dimensionless variable defined by Equation (35)
$\overline{R_{2s}}$	dimensionless variable defined by Equation (35)
$\overline{R_{3s,0}[Cl^-]}$	dimensionless variable defined by Equation (36)
$\overline{R_4}$	dimensionless variable defined by Equation (37)
S	variable defined by Equation (36)
S_c	the active site of the surface of cathode
U	variable defined by Equation (36)

W	variable defined by Equation (37)
X	variable defined by Equation (35)
Y	variable defined by Equation (35)
Z	variable defined by Equation (55)

Greek symbols

ϕ_2, ϕ_3, and ϕ_i	potential of the working electrode with respect to the reference electrode of reaction step (2), (3), and chain initiation
$\phi_{2,0}$, $\phi_{3,0}$, and $\phi_{i,0}$	equilibrium potential of the working electrode with respect to the reference electrode of reaction step (2), (3), and chain initiation
η_2, η_3, and η_i	overpotential of the electrode of reaction step (2), (3), and chain initiation
β_2, β_3, and β_i	transfer constants of the electrode of reaction step (2), (3), and chain initiation

1. Introduction

Trichloroethylene (TCE) is a commonly used industrial organic solvent; which is known to be toxic, while TCE waste is sometimes found as a contaminant in groundwater [1, 2]. Toxic metabolites, such as trichloroethanol and trichloroacetate are produced from the oxidative metabolism of TCE [3–5]. These compounds are known to be highly toxic and may cause secondary pollution. In order to eliminate the damage of these toxic metabolites contaminating the environment, TCE has been decomposed into CO_2 and other harmless species using biodegradation [6, 7] and photo-degradation [8–12].

Due to the potentially harmful properties of TCE, it is important to be able to monitor TCE concentrations for environmental protection. At present, the methods used to determine TCE concentration are gas chromatography (GC) [8], gas chromatography–mass spectrometry (GC–MS) [3, 5, 11], Fourier Transform infrared spectroscopy (FTIR) [9, 10], flow injection analysis (FIA) [7], and electrochemical sensor based methods [13–15]. Although the GC procedure is sensitive, it provides limited information about the individual molecular species. To improve on this situation, some researchers have used gas chromatography–mass spectrometry (GC–MS). This method can elucidate the relative amounts of the 'metabolites' of TCE, which can be identified using a full mass spectra scan for comparison with reference compounds. FTIR can both be used in qualitative and quantitative analyses of TCE, but the effect of humidity may adversely affect analytical accuracy. Volatilization needs to be suppressed during measurements with FIA in order to measure low concentrations of TCE. The system performance was evaluated with actual field samples, but FIA is limited in that it cannot detect high concentrations of TCE. Electrochemical sensors are convenient and sensitive but provide limited information about individual molecular metabolites.

In our research into the generation of TCE sensors, acetylene chloride, which can be produced by an electrochemical method [14] as shown in Equation (1) was thought to be an interesting material due to it having a large number of overtone and combination bands. The pure rotational spectrum of acetylene chloride has been examined [16–18]; this shows assignable vibration–rotation structure and some sensing devices have been developed using this information.

$$\mathrm{HClC{=}CCl_2} + 2\mathrm{e^-} \longrightarrow \mathrm{HC{\equiv}Cl} + 2\mathrm{Cl^-} \qquad (1)$$

The cathodic generated acetylene chloride can be used as a monomer for anodic polymerization as represented by Equation 2.

$$n\mathrm{HC{\equiv}Cl} \longrightarrow (-\mathrm{HC{=}CCl}-)_n \qquad (2)$$

A detailed reaction mechanism is proposed in this study and a mathematical function has been developed. In the previous study, it was reported that a very long linear conjugated polyene might have various interesting properties as represented by its optical, electrical and magnetic characteristics [19]. A polyene has an even number of methyne groups, which are covalently bonded to form a linear carbon chain bearing one pi-electron on each carbon atom [19]. An alternating conjugated system is a polymer produced from carbon–carbon triple bonds or with cumulated double bonds [20]. In this study, we used acetylene chloride as a monomer, with which to synthesize a novel conjugated polymer by electropolymerization.

Our theoretical analysis correlates well with the experimental results, and as such should prove useful in the development and the application of the conducting polymer described.

2. Reaction mechanism of paired electropolymerization

Reaction mechanisms that account for the cathodic reduction of TCE using Pd electrodes, and for the anodic polymerization of acetylene chloride polymer are proposed. At the beginning of the reaction, TCE is reduced on the Pd electrode in the cathodic system. TCE acquires two electrons from the cathode and loses two Cl^- ions. Equations (3) to (6), show the kinetics of TCE transfer to acetylene chloride:

$$HClC=CCl_2+Pb \underset{k_{-1}}{\overset{k_1}{\rightleftharpoons}} HClC=CCl_{2ads} \quad (3)$$

$$HClC=CCl_{2ads}+e^- \underset{k_{-2}}{\overset{k_2}{\rightleftharpoons}} HClC=CCl^-_{2ads} \quad (4)$$

$$HClC=CCl^-_{2ads}+e^- \underset{k_{-3}}{\overset{k_3}{\rightleftharpoons}} HClC=CCl^-+Cl^-+Pb \quad (5)$$

$$HClC=CCl^- \xrightarrow{k_4} ClC\equiv CH+Cl^- \quad (6)$$

For the main reaction, acetylene chloride monomers were produced in the cathodic system and transferred to the anodic system by agitation. In the anodic system, acetylene chloride loses a H^+ ion and then an electron is transferred to the anode to form a free radical, this initiation step is shown in Equations (7) to (8).

$$ClC\equiv CH \xrightarrow{k_5} ClC\equiv C^-+H^+ \quad (7)$$

$$ClC\equiv C^- \xrightarrow{k_i} ClC\equiv C^{\cdot}+e^- \quad (8)$$

The free radial species formed from acetylene chloride reacts with acetylene chloride monomers leading to the reactive propagation reaction steps, represented by Equations (9) to (11),

$$ClC\equiv C^{\cdot}+HC\equiv CCl \xrightarrow{k_p} ClC\equiv C-HC=CCl^{\cdot} \quad (9)$$

$$ClC\equiv C-HC=CCl^{\cdot}+HC\equiv CCl \xrightarrow{k_p} ClC\equiv C-HC=CCl-HC=CCl^{\cdot} \quad (10)$$

$$(ClC\equiv C)-(HC=CCl)^{\cdot}_{n-1}+HC\equiv CCl \xrightarrow{k_p} (ClC\equiv C)-(HC=CCl)^{\cdot}_{n} \quad (11)$$

When any two radials interact, the chain reaction is terminated as shown in Equations (12) to (13).

$$(ClC\equiv C)-(HC=CCl)^{\cdot}_{n}+(ClC\equiv C)-(HC=CCl)^{\cdot}_{m} \xrightarrow{k_t} (ClC\equiv C)-(HC=CCl)_{n+m}-(C\equiv CCl) \quad (12)$$

$$2ClC\equiv C^{\cdot} \xrightarrow{k_{t1}} ClC\equiv C-C\equiv CCl \quad (13)$$

Side reactions of TCE potentially occur at the anode, where the free radial from TCE is transferred from bulk to anode during TCE decomposition. A H^+ ion diffuses into the bulk solution and an electron transfers from the $Cl_2C=CCl^-$ species to the anode and forms a free radical $Cl_2C=CCl\cdot$, which is a means of initiation that can start another chain reaction.

$$HClC=CCl_2 \xrightarrow{k_{s1}} Cl_2C=CCl^-+H^+ \quad (14)$$

$$Cl_2C=CCl^- \xrightarrow{k_{si}} Cl_2C=CCl^{\cdot}+e^- \quad (15)$$

The free radial form of TCE reacts with TCE to sustain propagation of the side reactions as shown in Equations (16) and (17).

$$Cl_2C=CCl^{\cdot}+HClC=CCl_2 \xrightarrow{k_{sp}} Cl_2C=CCl-HClC-CCl^{\cdot}_2 \quad (16)$$

$$Cl_2C=CCl-(ClHC-CCl_2)^{\cdot}_{n-1}+ClHC=CCl_2 \xrightarrow{k_{sp}} (Cl_2C=CCl)-(HClC-CCl_2)^{\cdot}_{n} \quad (17)$$

When two free radials of reactive intermediates, or two free radials of TCE collide, the termination of the reaction occurs as shown by Equations (18) and (19).

$$(Cl_2C=CCl)-(HClC-CCl_2)^{\cdot}_{n}+(Cl_2C=CCl)-(HClC-CCl_2)^{\cdot}_{m} \xrightarrow{k_{st}} (Cl_2C=CCl)-(HClC-CCl_2)_{n+m}-(ClC=CCl_2) \quad (18)$$

$$2Cl_2C=CCl^{\cdot} \xrightarrow{k_{st1}} Cl_2C=CCl-ClC=CCl_2 \quad (19)$$

In general, the degree of dissociation shown in Equation (7) is much greater than that in Equation (14), and the main reaction is advantaged relative to the side reaction.

3. Kinetic analysis

The kinetic analysis can be represented as, Equations (3) to (19); following on from this:

In the cathodic system,

$$R_1+S_c \underset{k_{-1}}{\overset{k_1}{\rightleftharpoons}} R_{1s} \quad (20)$$

where S_c is surface of cathode, and R_{1s} is $HClC=CCl_{2ads}$.

$$R_{1s}+e^- \underset{k_{-2}}{\overset{k_2}{\rightleftharpoons}} R_{2s} \quad (21)$$

where R_{2s} is $HClC=CCl^-_{2ads}$.

$$R_{2s}+e^- \underset{k_{-3}}{\overset{k_3}{\rightleftharpoons}} R_{3s}+Cl^- \quad (22)$$

where R_{3s} is $HClC=CCl^-_{ads}$.

$$R_{3s} \xrightarrow{k_4} M+Cl^- \quad (23)$$

where M is HC ≡ CCl.

In the anodic system where the side reaction was negleted, M decomposes into R_4 and a H^+ ion,

$$M \xrightarrow{k_5} R_4 + H^+ \tag{24}$$

where R_4 is ClC ≡ C$^-$.

When an electron was removed from R_4 and a free radical N· was formed, the chain initiation was initiated by this free radical,

$$R_4 \xrightarrow{k_i} N^{\cdot} + e^- \tag{25}$$

where N· is ClC ≡ C·.

Then N· reacts with acetylene chloride monomers to induce the reactive propagation as shown in Equations (26) to (28).

$$N^{\cdot} + M \xrightarrow{k_{p1}} NM^{\cdot} \tag{26}$$

$$NM^{\cdot} + M \xrightarrow{k_p} NM_2^{\cdot} \tag{27}$$

$$NM_{n-1}^{\cdot} + M \xrightarrow{k_p} NM_n^{\cdot} \tag{28}$$

where NM_n· is (ClC ≡ C)–(HC = CCl)$_n$ ·

The collision of two intermediate free radicals, or of TCE would lead to the termination of the reaction:

$$NM_n^{\cdot} + NM_m^{\cdot} \xrightarrow{k_t} NM_{n+m}N \tag{29}$$

$$NM_n^{\cdot} + N^{\cdot} \xrightarrow{k_{t1}} N_2M_n \tag{30}$$

where NM_{n+m} N is (ClC ≡ C)–(HC = CCl)$_{n+m}$ –(C ≡ CCl)

$$N^{\cdot} + N^{\cdot} \xrightarrow{k_{t2}} NN \tag{31}$$

where: NN is ClC ≡ C–C ≡ CCl.

Kinetic analysis based on the Butler–Volmer equation [21, 22] gives the current density for Equation (21) which is expressed here as Equation (32).

$$\begin{aligned} i_2 &= Fk_2R_{1s}\exp(-\beta_2F\phi_2/RT) \\ &\quad - Fk_{-2}R_{2s}\exp[(1-\beta_2)F\phi_2/RT] \end{aligned} \tag{32}$$

At equilibrium,

$$\phi_2 = \phi_{2,0} \tag{33}$$

Therefore the exchange current density corresponding to Equation (32) is given by Equation (34).

$$\begin{aligned} i_{2,0} &= Fk_2R_{1s,0}\exp(-\beta_2F\phi_{2,0}/RT) \\ &= Fk_{-2}R_{2s,0}\exp[(1-\beta_2)F\phi_{2,0}/RT] \end{aligned} \tag{34}$$

From Equations (32) and (34), we obtain

$$\begin{aligned} i_2 &= i_{2,0}\left\{\frac{R_{1s}}{R_{1s,0}}\exp[-\beta_2F(\phi_2-\phi_{2,0})/RT]\right. \\ &\quad \left. - \frac{R_{2s}}{R_{2s,0}}\exp[(1-\beta_2)F(\phi_2-\phi_{2,0})/RT]\right\} \\ &= i_{2,0}\left[\overline{R_{1s}}X - \overline{R_{2s}}Y\right] \end{aligned} \tag{35}$$

where $\overline{R_{1s}} = \frac{R_{1s}}{R_{1s,0}}$, $\overline{R_{2s}} = \frac{R_{2s}}{R_{2s,0}}$, $\eta_2 = \phi_2 - \phi_{2,0}$, $X = \exp[-\beta_2 F(\phi_2 - \phi_{2,0})/RT] = \exp(-\beta_2 F\eta_2/RT)$, and $Y = \exp[(1-\beta_2)F(\phi_2 - \phi_{2,0})/RT] = \exp[(1-\beta_2)F\eta_2/RT]$.

Similarly, Equation (22) can be expressed as

$$\begin{aligned} i_3 &= i_{3,0}\left\{\frac{R_{2s}}{R_{2s,0}}\exp[-\beta_3F(\phi_3-\phi_{3,0})/RT] - \frac{R_{3s}[Cl^-]}{R_{3s,0}[Cl^-]_0}\right. \\ &\quad \left. \times \exp[(1-\beta_3)F(\phi_3-\phi_{3,0})/RT]\right\} \\ &= i_{3,0}\left[\overline{R_{2s}}U - \overline{R_{3s,0}[Cl^-]}S\right] \end{aligned} \tag{36}$$

where $\overline{R_{2s}} = \frac{R_{2s}}{R_{2s,0}}$, $\overline{R_{3s,0}[Cl^-]} = \frac{R_{3s}[Cl^-]}{R_{3s,0}[Cl^-]_0}$, $\eta_3 = \phi_3 - \phi_{3,0}$, $U = \exp[-\beta_3 F(\phi_3 - \phi_{3,0})/RT] = \exp(-\beta_3 F\eta_3/RT)$, and $S = \exp[(1-\beta_3)F(\phi_3 - \phi_{3,0})/RT] = \exp[(1-\beta_3)F\eta_3/RT]$

Similarly, Equation (25) can be expressed as

$$\begin{aligned} i_i &= i_{i,0}\left\{\frac{R_4}{R_{4,0}}\exp[-\beta_iF(\phi_i-\phi_{i,0})/RT] - \frac{N^{\cdot}}{(N^{\cdot})_0}\right. \\ &\quad \left. \times \exp[(1-\beta_i)F(\phi_i-\phi_{i,0})/RT]\right\} \\ &= i_{i,0}\left[\overline{R_4}P - \overline{N^{\cdot}}W\right] \end{aligned} \tag{37}$$

where $\overline{R_4} = \frac{R_4}{R_{4,0}}$, $\overline{N^{\cdot}} = \frac{N^{\cdot}}{(N^{\cdot})_0}$, $\eta_i = \phi_i - \phi_{i,0}$, $P = \exp[-\beta_iF(\phi_i - \phi_{i,0})/RT] = \exp(-\beta_iF\eta_i/RT)$, and $W = \exp[(1-\beta_i)F(\phi_i - \phi_{i,0})/RT] = \exp[(1-\beta_i)F\eta_i/RT]$

The total current density at the cathode and anode, respectively, is:

$$\begin{aligned} i &= i_2 + i_3 = i_i \\ &= i_{2,0}[\overline{R_{1s}}X - \overline{R_{2s}}Y] + i_{3,0}[\overline{R_{2s}}U - \overline{R_{3s,0}}[Cl^-]S] \\ &= i_{i,0}[\overline{R_4}P - \overline{N^{\cdot}}W] \end{aligned} \tag{38}$$

Based on material balance and at steady state, shown in Equation (21), we obtain

$$\frac{dR_{2s}}{dt} = \frac{i_2}{F} - \frac{i_3}{F} = 0 \Rightarrow i_2 = i_3 \tag{39}$$

Substituting Equation (39) into Equation (38), the general rate equation of the proposed reaction mechanism is obtained as

$$i = 2i_2 = 2i_{2,0}[\overline{R_{1s}}X - \overline{R_{2s}}Y] = i_i = i_{i,0}[\overline{R_4}P - \overline{N^{\cdot}}W] \tag{40}$$

At steady state

$$\frac{dR_{1s}}{dt} = k_1 R_1 C_v - k_{-1} R_{1s} - k_2 R_{1s} X + k_{-2} R_{2s} Y = 0 \quad (41)$$

where, C_v is unoccupied active site on the cathodic surface, which is not covered by any adsorbing species. Similarly, the material balances of the other species are:

$$\frac{dR_{2s}}{dt} = k_2 R_{1s} X - k_{-2} R_{2s} Y - k_3 R_{2s} U + k_{-3} R_{3s} [Cl^-] S = 0 \quad (42)$$

$$\frac{dR_{3s}}{dt} = k_3 R_{2s} U - k_{-3} R_{3s} [Cl^-] S - k_4 R_{3s} = 0 \quad (43)$$

$$\frac{dR_4}{dt} = k_5 M - k_i R_4 = 0 \quad (44)$$

$$\frac{dM}{dt} = k_4 R_{3s} - k_5 M - k_p (NM_n^{\cdot}) M - k_p (NM_n^{\cdot}) M \quad (45)$$

$$\frac{dN^{\cdot}}{dt} = k_i R_4 - k_{p1} N^{\cdot} M^{\cdot} - k_{t1} NM_n^{\cdot} N^{\cdot} - k_{t2} N^{\cdot} N^{\cdot} = 0 \quad (46)$$

$$\frac{dNM_n^{\cdot}}{dt} = k_{p1} N^{\cdot} M - k_t NM_n^{\cdot} NM_m^{\cdot} - k_{t1} NM_n^{\cdot} N^{\cdot} = 0 \quad (47)$$

$$\frac{dNM_{n+m}N^{\cdot}}{dt} = k_t NM_n^{\cdot} NM_m^{\cdot} = 0 \quad (48)$$

By adding Equation (41) to (43) we obtain

$$R_{3s} = [k_1 R_1 C_v - k_{-1} R_{1s}]/k_4 \quad (49)$$

From Equations (41), R_{2s} is obtained

$$R_{2s} = [(k_{-1} + k_2 X) R_{1s} - k_1 R_1 C_v]/k_{-2} Y \quad (50)$$

Substituting Equations (49) and (50) into Equation (42), gives

$$C_v = R_{1s} \frac{[k_{-1} + \frac{k_{-1}k_2k_3XU}{k_{-2}Y} + \frac{k_{-1}k_{-3}S[Cl^-]}{k_4}]}{k_1 R_1 + \frac{k_1 k_3 R_1 U}{k_{-2}Y} + \frac{k_1 k_{-3} R_1 S[Cl^-]}{k_4}} = R_{1s}/A \quad (51)$$

where

$$A = \frac{k_1 R_1 + \frac{k_1 k_3 R_1 U}{k_{-2}Y} + \frac{k_1 k_{-3} R_1 S[Cl^-]}{k_4}}{k_{-1} + \frac{k_{-1}k_2k_3XU}{k_{-2}Y} + \frac{k_{-1}k_{-3}S[Cl^-]}{k_4}} \quad (52)$$

The total active sites on the cathodic surface, C_t, is

$$C_t = C_v + R_{1s} + R_{2s} + R_{3s} \quad (53)$$

Substituting Equations(49) and (50) into Equation(53), we obtain the total active sites on the cathode surface, C_t as

$$C_t = [1 + 1/A + (k_{-1} + k_2 X)/k_{-2} Y - (k_1 R_1/k_{-2} YA) + (k_1 R_1/k_4 A) - k_{-1}/k_4] R_{1s} = R_{1s} Z \quad (54)$$

where

$$Z = [1 + 1/A + (k_{-1} + k_2 X)/k_{-2} Y - (k_1 R_1/k_{-2} YA) + (k_1 R_1/k_4 A) - k_{-1}/k_4] \quad (55)$$

At large overpotential $X \gg Y$, Equation (40) becomes

$$i = 2i_{2,0}(\overline{R_{1s}} X) = 2_{i2,0} \frac{R_{1s}}{R_{1s,0}} X \quad (56)$$

Substituting Equation (54) into Equation (56) gives

$$i = \frac{2i_{2,0} X C_t}{R_{1s,0} Z} \quad (57)$$

For the cathodic reaction, we assume $k_2 \gg k_{-1}$, $k_3 \gg k_{-2}$, $k_4 \gg k_{-3}$, then Equations (52) and (55) become

$$A = (k_1 R_1/k_{-1} k_2 X) \quad (58)$$

$$Z = 1 + k_{-1} k_2 X/k_1 R_1 + k_{-1} k_2 X/k_4 \quad (59)$$

Substituting Equation (59) into Equation (57)

$$i = \frac{2i_{2,0} X C_t}{R_{1s,0} Z} = \frac{2i_{2,0} X C_t}{R_{1s,0}\left(1 + \frac{k_{-1}k_2X}{k_1R_1} + \frac{k_{-1}k_2X}{k_4}\right)} \quad (60)$$

Equation (60) can be simplified as follows:

Case I: If Equation (20) is the rate determining step, $k_1 \ll k_2$, k_3, k_4, respectively where it is assumed that $\frac{k_{-1}k_2X}{k_1R_1} \gg 1 + \frac{k_{-1}k_2X}{k_4}$, the current density of Equation (60) becomes

$$i = \frac{2i_{2,0} k_1 R_1 C_t}{R_{1s,0} k_{-1} k_2} \quad (61)$$

Case II: If equation (21) is the rate determining step, $k_2 \ll k_1$, k_3, k_4, respectively, we can assume, $1 \gg \frac{k_{-1}k_2X}{k_4} + \frac{k_{-1}k_2X}{k_1R_1}$, then equation (60) becomes

$$i = \frac{2i_{2,0} X C_t}{R_{1s,0}} \quad (62)$$

Case III: If equation (22) is the rate determining step, $k_3 \ll k_1$, k_2, k_4, respectively, equation (60) becomes

$$i = \frac{2i_{2,0} X C_t}{R_{1s,0}\left(1 + \frac{k_{-1}k_2X}{k_1R_1} + \frac{k_{-1}k_2X}{k_4}\right)} \quad (63)$$

Case IV: If equation (23) is the rate determining step, $k_4 \ll k_1$, k_2, k_3, respectively, equation (60)

$$i = \frac{2i_{2,0} k_4 C_t}{R_{1s,0} k_{-1} k_2} \quad (64)$$

A summary of the case study is shown in Table 1.

Table 1. Summary of case study

Rate determining step	Current density equation $i = \frac{2i_{2,0}XC_t}{R_{1s,0}Z} = i_{1,0}[\overline{R_4}P - \overline{N} \cdot W]$
Equation (20)	$i = \frac{2i_{2,0}k_1R_1C_t}{R_{1s,0}k_{-1}k_2}$
Equation (21)	$i = \frac{2i_{2,0}XC_t}{R_{1s,0}}$
Equation (22)	$i = \frac{2i_{2,0}XC_t}{R_{1s,0}(1+\frac{k_{-1}k_2X}{k_1R_1}+\frac{k_{-1}k_2X}{k_4})}$
Equation (23)	$i = \frac{2i_{2,0}k_4C_t}{R_{1s,0}k_{-1}k_2}$

4. Experimental

The electrolysis system comprised three electrodes, namely: working, counter and reference electrodes, which were an electrodeposited Pd electrode, a Pt electrode and a liquid junction Ag/Ag^+ electrode (with 0.1 M tetrabutylammonium perchlorate (TBAP) in acetonitrile), respectively. Power settings were controlled by a potentiostat/galvanostat (EG&G model 263). The TBAP and AN were purched from TCI (Japan) and Tedia (USA), respectively. The reaction volume was 50 ml (0.01 M of the organic electrolyte tetrabutylammonium tetrafluoroborate (TBAT, TCI, Japan) in AN solution), which was agitated by a magnetic stirrer at 155 rpm at room temperature. The polymerization of acetylene chloride was able to be cathodically achieved from different concentrations of TCE (Aldrich, USA). The electropolymerization was carried out at applied potentials from 1.8 to 2.1 V vs Ag/Ag^+ in the reactive electrolyte.

The scheme of paired-electrochemical reactions in TCE solution is shown in Fig. 1. The characteristics of the products was described previously [14].

The procedure for preparing a working electrode was as follows: A graphite stick ($1 \times 6 \times 0.3$ cm, ED-11 model, purchased from Center Carbon Company, Taiwan), was cut and Pd deposited in an area of 1.5 cm^2 controlled by parafilm tape. The graphite stick was used as a substrate for electrodeposition of Pb. The working electrode was ultrasonically cleaned in 0.1 M HNO_3 aqueous solution and was thoroughly washed with deionized (DI) water. Then the graphite stick substrate was immersed in the electrodeposited Pb aqueous solution containing 0.63 M lead(II) tetrafluoroborate ($Pb(BF_4)_2$, Alfa Aesar, USA), 0.68 M tetrafluoroboric acid (HBF_4, Rieded-deHaën, Germany), 0.43 M boric acid (H_3BO_3, Rieded-deHaën, USA) and 0.0006 M polyethylene glycol (PEG300, Hayashi, Japan). Finally, the electrodeposition of Pb for preparing the working

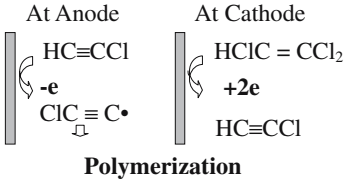

Fig. 1. Basis of paired-electrochemical reaction in TCE solution.

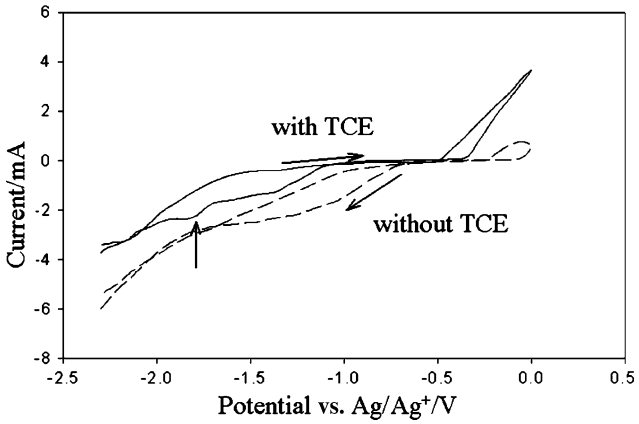

Fig. 2. The cyclic-voltammograms of electrodeposited Pb modified electrode with and without TCE in the 0.01 M TBAT organic electrolyte.

electrode was carried out at 100 rpm agitation rate at room temperature. The electrodeposition current density was 40 mA cm^{-2} and the duration was 2 h.

5. Results and discussion

The cyclic-voltammograms of electrodeposited Pb modified electrode with and without TCE in the 0.01 M TBAT organic electrolyte are shown in Fig. 2. The main reduction peak appears at −1.8 V (vs. Ag/Ag^+) and indicates that the reduction of TCE occurs on the surface of electrodeposited Pb modified electrode in the organic electrolyte.

The relationship between current density and potential at different concentrations of TCE are shown in Fig. 3. The results show the current density increases, both with the applied potential at fixed concentrations

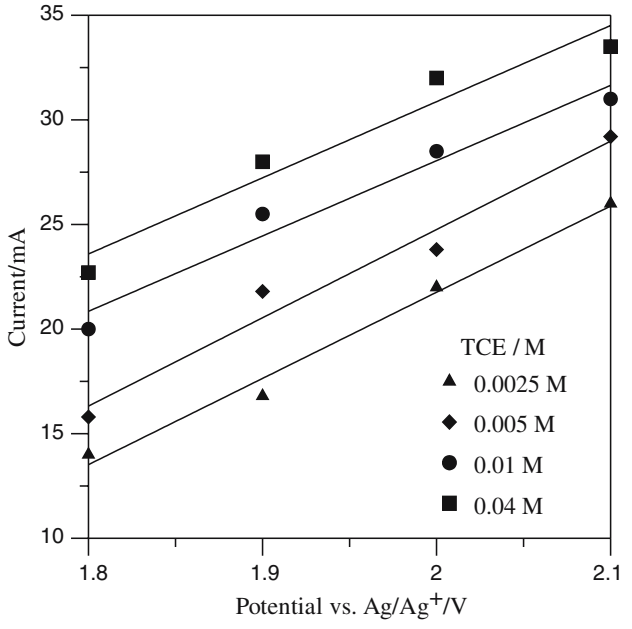

Fig. 3. I.E. curve of TCE reduction for the paired electrolysis.

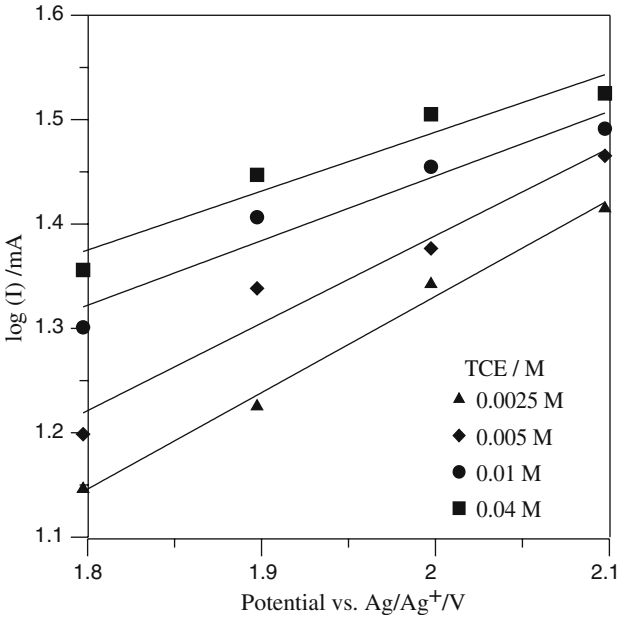

Fig. 4. The Tafel plot of TCE reduction for the electrolysis.

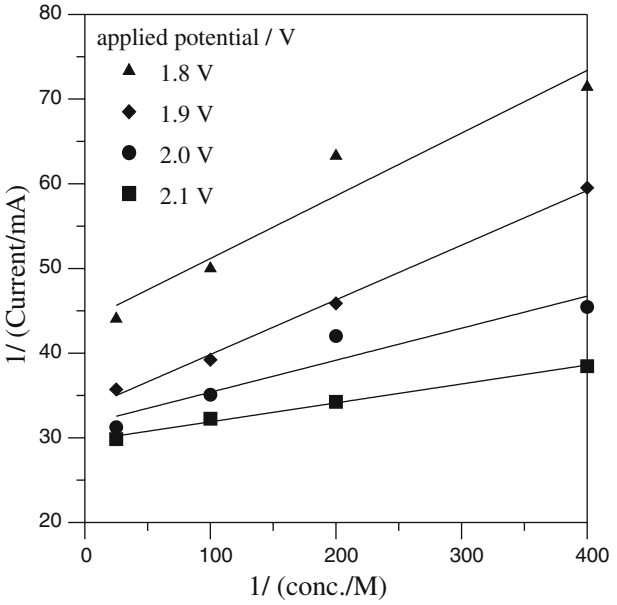

Fig. 5. The reciprocal plot of current density against concentration of TCE.

of TCE and with the concentration of TCE at a fixed applied potential.

The Tafel curves at different concentrations of TCE are shown in Fig. 4. The Tafel curves change with TCE concentrations and a linear section of each Tafel curve was obtained. As shown in Table 2, the slopes of the straight lines change from 923.6 to 565 mV. The transfer coefficient, β_2, increases with the concentration of TCE. The average transfer coefficient was 0.0835.

The reciprocal plot of current density against the concentration of TCE is shown in Fig. 5. Equation (63) of the kinetic analysis section can be represented as $\frac{1}{i} = \frac{R_{1s,0}k_{-1}k_2}{2i_{2,0}C_t k_1 X}\left(\frac{1}{R_1} + \frac{k_1}{k_{-1}k_2 X} + \frac{k_1}{k_4}\right)$ which can be compared with the plots of Fig. 5. The kinetic analysis of Equation (63) correlate well with the experiment results. The analyses of the kinetic parameters are shown in Table 3. The kinetic parameter, $\frac{R_{1s,0}}{2i_{2,0}C_t}$, under different concentrations of TCE and applied potentials, distributes from 78.79 to 62.27 and the average value is 66.92.

Table 3. Analysis of kinetic parameters

E/V	$\frac{R_{1s,0}k_{-1}k_2}{2i_{2,0}C_t k_1}$	$\frac{k_1}{k_{-1}k_2X} + \frac{k_1}{k_4}$	$\frac{k_1}{k_{-1}k_2}$	$\frac{R_{1s,0}}{2i_{2,0}C_t}$
1.8	0.074	591.13	1064.04	78.79
1.9	0.0646	517.05	982.39	63.42
2.0	0.0378	835.04	1670.09	63.19
2.1	0.0223	1326.86	2786.40	62.27

6. Conclusions

A reaction mechanism to account for the paired-electropolymerization of trichloroethylene has been proposed and a theoretical kinetic analysis of the proposed reaction mechanism has been derived. The general reaction equation was also obtained.

Table 2. Tafel slope of TCE

Concentration of TCE/M	Tafel slope/mV	Transfer Coefficient (β_2)
0.0025	923.6	0.064
0.005	838.3	0.070
0.01	619.3	0.095
0.04	565.0	0.105

Case III of the theoretical analysis correlated well with the experimental results. The rate determining step was found to be the cathodic reduction of $HClC{=}CCl_2^-$ to $HClC{=}CCl^-$ and the Cl^- ion. The paired electrolysis current of TCE can be expressed as:

$$\frac{1}{i} = 0.0497\frac{1}{[\mathrm{TCE}]} + 66.92\frac{1}{X}. \tag{64}$$

Acknowledgements

The support of the Program for Promoting Acdemic Excellence of Universities (EX-91-E-FA09-5-4) from the ministry of Education of the Republic of China and National Cheng Kung University are gratefully acknowledged.

References

1. Y. Morioka, *J. Jpn. Soc. Water Eniviron.* **19** (1996) 529.
2. K.H. Wang, H.H. Tsai and Y.H. Hsieh, *Appl. Catal. B Environ.* **17** (1998) 313.
3. T.Q. Shang, S.L. Doty, A.M. Wilson, W.N. Howald and M.P. Gordon, *Phytochem* **58** (2001) 1055.

4. P.G. Forkert, L.H. Lash, V. Nadeau, R. Tardif and A. Simmonds, *Toxicol. Appl. Pharmacol.* **182** (2002) 244.
5. J.Z. Song and J.W. Ho, *J. Chromatogr. B.* **789** (2003) 303.
6. Y. Nakano, L.Q. Hua, W. Nishijima, E. Shoto and M. Okada, *Water Res.* **34** (2000) 4139.
7. T.S. Han, S. Sasaki, K. Yano, K. Ikebukuro, A. Kitayama, T. Nagamune and I. Karube, *Talanta* **57** (2002) 271.
8. Y. Ku, C.M. Ma and Y.S. Shen, *Appl. Catal. B: Environ.* **34** (2001) 181.
9. P.B. Amama, K. Itoh and M. Murabayashi, *J. Mol. Catal. A: Chem.* **176** (2001) 165.
10. H. Joo, H. Jeong, M. Jeon and I. Moon, *Solar Energy Mater. Solar Cells* **79** (2003) 93.
11. T.H. Lim and S.D. Kim, *Chemosphere* **54** (2004) 305.
12. Z. Li, *Chemosphere* **54** (2004) 419.
13. M.H. Chen, T.Y. Lin and T.C. Chou, *J. Electrochem. Soc.* **149** (2002) H87.
14. M.H. Chen and T.C. Chou, *J. Electrochem. Soc.* **150** (2003) H214.
15. M.H. Chen, C.C. Liu and T.C. Chou, *Biosens. Bioelectron.* **20** (2004) 25.
16. G.R. Hunt and M.K. Wilson, *J. Chem. Phys.* **34** (1961) 1301.
17. M. Le Guennec, G. Wlodarczak and J. Demaison, *J. Mol. Spectrosc.* **158** (1993) 357.
18. D. McNaughton and M. Shallard, *J. Mol. Spectrosc.* **165** (1994) 185.
19. H. Shirakawa, *Rev. Mod. Phys.* **73** (2001) 713.
20. M. Kijima, I. Kinoshita, T. Hattori and H. Shirakawa, *Synth. Met.* **100** (1999) 61.
21. T.C. Chou, W.J. Chen, H.J. Tien and J.J. Jow, *Electrochim. Acta* **30** (1985) 1665.
22. J.J. Jow and C.C. Chou, *Electrochim. Acta* **32** (1987) 311.